Synthesis and Characterization of Poly(*o*-chloroaniline)/TiO₂ Nanocomposites for Photocatalytic Degradation of Direct Yellow 50 Dye in Textile Wastewater

Mirza Nadeem Ahmad[1],*, Muhammad Masood ul Hassan[1], Faisal Nawaz[2], Muhammad Naveed Anjum[1], Shahzad Zafar Iqbal[1], Tajamal Hussain[3], Adnan Mujahid[3], Muhammad Fayyaz Farid[1]
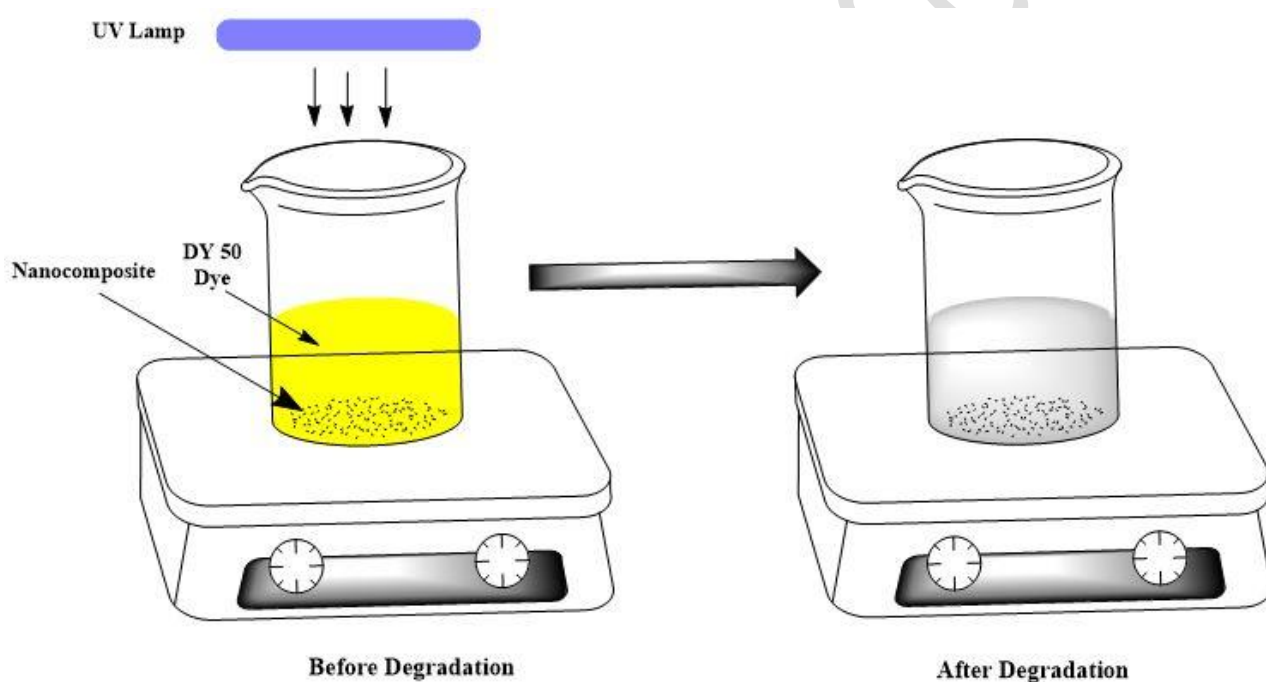
[1]Department of Applied Chemistry, Government College University Faisalabad 38000, Pakistan.

[2]University of Engineering and Technology, Lahore 54000, Pakistan

[3]School of Chemistry, University of Punjab Lahore 54000, Pakistan.

Corresponding author: mirzanadeemahmad@gcuf.edu.pk

GRAPHICAL ABSTRACT

Abstract

The nanocomposites of poly(*o*-chloroaniline) with titanium dioxide have been prepared via chemical oxidative polymerization technique using *o*-chloroaniline as monomer and titanium dioxide nanoparticles for photocatalytic application. The different composites were prepared by varying the load percentage of titanium oxide nanoparticles (TiO₂ NPs) in polyorthochloroaniline (POCA) matrix. The synthesized composite materials were characterized by Scanning electron microscopy (SEM), X-Rays diffraction (XRD), and Fourier transform infrared spectroscopy (FTIR)

techniques. The POCA/TiO$_2$ nanocomposites were further applied to evaluate the photocatalytic degradation potential towards direct yellow 50 (DY50) dye in textile wastewater under ultraviolet radiations.

1. Introduction

Water pollution is rising due to textile industry discharging a large proportion of effluent which comprises of synthetic dyes. Dyes that are synthesized have been widely utilized in the textile industries because of their cost effectiveness in production, easily available in large quantity, good stability to light, heat resistance, and advancement in colour covering the whole spectrum of colour. However, they are carcinogenic, non-biodegradable, toxic, mutagenic leading to various human health problems like skin cancer and other allergic effects (Madhav *et al.,* 2018). Such side effects of synthetic dyes compelled the researcher to think about more environment friendly and renewable sources of dyes to minimize the negative environmental impact of synthetic colourants (Huang *et al.,* 2016). Therefore, strict environmental and ecological legislation have been forced by various countries including European Union, USA, Germany and India. As a result, non-toxic and environment friendly naturally occurring bio-colourants have picking up reappearance as an ensuing substitute through green chemistry with widespread appropriateness to textile dying and other biomedical features. So, they divert again towards natural dyes (Kaounides *et al.,* 2007).

Many methods such as physical, biological and chemical have been used for the removal and degradation of dyes (organic dye) of different types from wastewater. Recently various techniques have been developed for this purpose such as Separation by using membrane, Chemical oxidation (Nguyen *et al.,* 2021), Adsorption (Badvi *et al.,* 2021), Degradation using microbes (Oon *et al.,* 2021), Electrochemical method (Belal *et al.,* 2021), Photocatalytic method (Vijayaraghavan *et al.,*

2021) and Coagulation (Eslami *et al.,* 2021). All these methods are successful and widely used all over the world for the treatment of dyes (Lee *et al.,* 2020).

Photocatalysis is the method in which the rate of photoreaction increases due to the availability of a catalyst. Different metallic oxides such as zinc oxide, TiO_2 and etc. are utilized as catalyst in photocatalysis (M. B. Nguyen *et al.,* 2021; Ramamoorthy *et al.,* 2021). The function of a catalyst is to generate pairs of electron-hole which produce free radicals like hydroxyl free radicals. The efficiency of a photocatalyzed reaction depends upon the efficiency of the catalyst to produce electron-hole pairs. During the photocatalysis, light is absorbed by the substrate molecules. In 1972, advance oxidative process was discovered by Honda and Fujishima. This process was later called photocatalysis. Semiconductors were first used for water splitting reactions. But later, they were used as catalysts (Barzegar *et al.,* 2021; Chen *et al.,* 2017). It has been later discovered that this technology was energy saving, sustainable and environment friendly (Ali *et al.,* 2020).

Nanocomposites are those materials that are synthesized at nanometer scale by mixing different materials and form a large variety of systems such as one-dimensional, two-dimensional and three dimensional. The most important class of nanocomposites is that in which organic/inorganic materials are used. The properties of nanocomposites do not only depend on their individual parents but also on their interfacial characteristics and morphology. Zeolite is an example of three-dimensional framework system which is made up of inorganic composites. Clay, metal oxide, metal phosphate and chalcogenides are examples of two-dimensional systems. There is one-dimensional system such as $(Mo_3Se_3^-)_n$ chains and zero-dimensional as clusters (Noman *et al.,* 2020).

TiO_2 is modified in such a way that it becomes active in the presence of ultraviolet light. This modified TiO_2 was used in the construction of concrete structures by the European Commission. TiO_2 becomes active by the absorption of UV light and degrade harmful pollutants such as NO and NO_2 through photocatalysis and converted them into harmless substances such as NO_3 (Rouzafzay *et al.,* 2020). Antifouling coatings have been synthesized which are extensively used as a

photocatalyst as well as separating layers. Titanium dioxide photocatalyst is used for the disinfection of water. Titanium oxide produces free radicals which oxidize the organic matter. Moreover, titanium oxide is also used in self-cleaning glass (Rani *et al.,* 2020).

In polymer nanocomposites, the organic polymers are coated on the inorganic nanoparticles. When the polymer is coated on the nanoparticles, they are called core-shell structures. After the polymerization of monomers, nanoparticles are dispersed in the polymer which act as dispersed phase and polymer acts as a matrix. Due to its high surface to volume ratio, they are unstable and tend to aggregate. Due to agglomeration, their surface to volume ratio decreases and its efficiency and quality is also reduced. These nanoparticles are unstable because they are oxidized and the properties of parent nanoparticles are modified. In order to avoid such disadvantages, nanoparticles are dispersed into the synthetic and natural polymers. These polymer nanocomposites are synthesized in two ways, by dispersion during the polymerization and dispersion of nanoparticles in the preformed polymer (Sarkar *et al.,* 2012).

Therefore, the current research work was designed to prepare the poly(o-chloroaniline)/TiO$_2$ nanocomposites and study their photocatalytic activity by the degradation of direct yellow 50 dye.

2. MATERIALS AND METHODS

2.1 Reagents and Chemical

Analytical grade chemicals and reagents were used for this research work mainly consisting of *o*-chloroaniline monomer, Hydrochloric acid (HCL), Potassium per-sulphate (KPS) (K$_2$S$_2$O$_8$), Distilled water and Ethanol (C$_2$H$_5$OH). All the chemicals were used as received. Wastewater containing direct yellow 50 dye was collected from Five-Star Textile Industry Maqbool Rd, Batala Colony, Faisalabad, Pakistan.

2.2 Methodology

2.2.1 Synthesis of TiO$_2$ NPs

Titanium dioxide nanoparticles were synthesized by acetic acid hydrolysis process using standard reported method (Konstantinou *et al.,* 2004). Acetic acid (1 M) was dissolved in distilled water and stirred for 30 minutes. Titanium isopropoxide (0.5 M) was added to acetic acid solution and stirred for 6 hours at 50 °C. The dispersion was then centrifuged at 5000 rpm for 10 minutes to collect the nanoparticles. They were then dried in an electric oven at 80 °C.

2.3 Synthesis of TiO$_2$/POCA nanocomposites

TiO$_2$/POCA nanocomposites were prepared in three different compositions which are as follows:

Table 1: Compositions of POCA/TiO$_2$ Nanocomposites

Sample name	POCA	TiO$_2$	Ratio
Composition 1 (S1)	2ml	10g	1:5
Composition 2 (S2)	2ml	5g	2:5
Composition 3 (S3)	2ml	20g	1:10

2.4 Procedure

The nanocomposites of three different compositions were prepared. For this purpose, first of all, 4 molar solution of HCL was prepared in distilled water. Then, for sample 1 (10g) of TiO$_2$ powder, for sample 2 (5g) and for sample 3 (20g) of TiO$_2$ powder was used. Further, 100 ml of 1M HCl was taken in a beaker and TiO$_2$ powder was dispersed in this solution by magnetic hotplate for 10 minutes. This allowed the powder to completely disperse in HCl solution. Further, 2 ml of *o-*

chloroaniline was added in the dispersion. Then, another beaker was filled with 25 ml of distilled water and 5g of potassium persulphate (KPS) was prepared as oxidant. Subsequently, oxidant was added to the dispersion drop wise with constant stirring for 3 hours. A green coloured gel was obtained which was centrifuged and washed with water and ethanol several times. The obtained gel was then dried in the electric oven at 80 ºC and which converted into fine powder on drying.

3. Results and discussion

3.1 Fourier-transform Infrared Spectroscopy (FTIR)
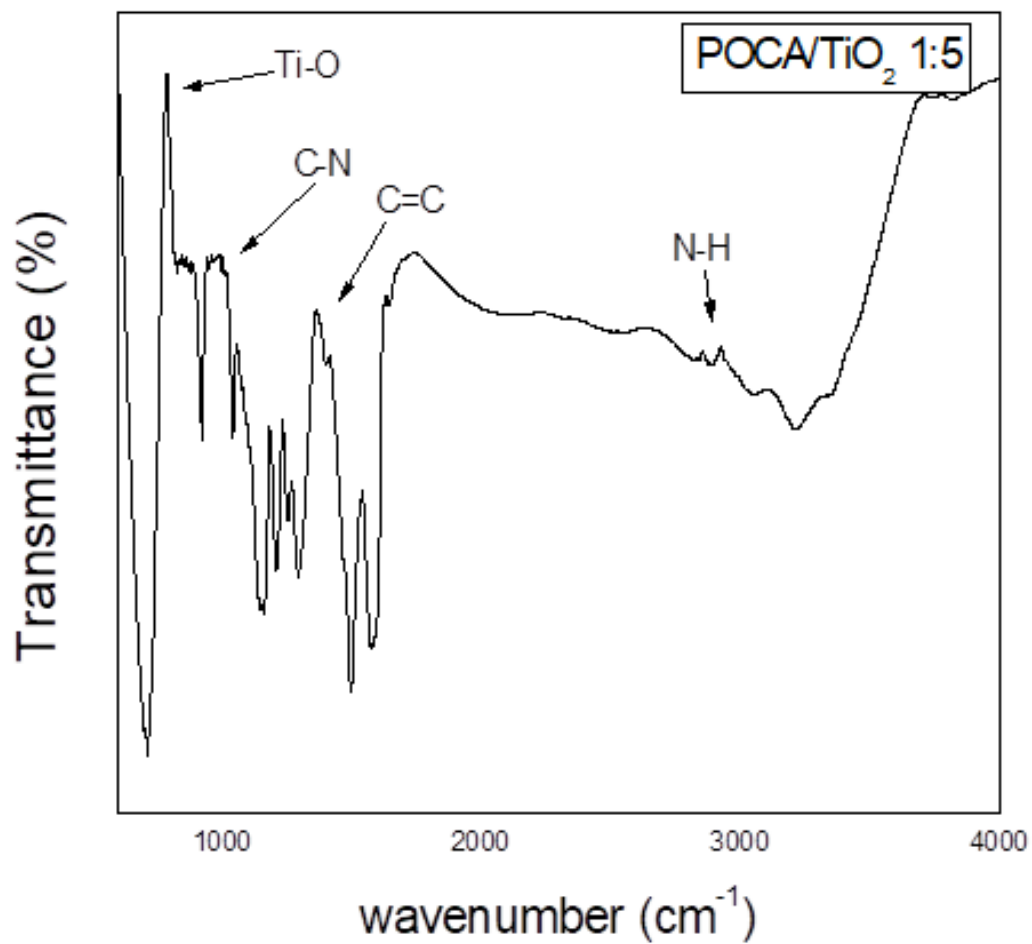
Fig 3.1 FTIR spectra of POCA/TiO$_2$ sample (S1)
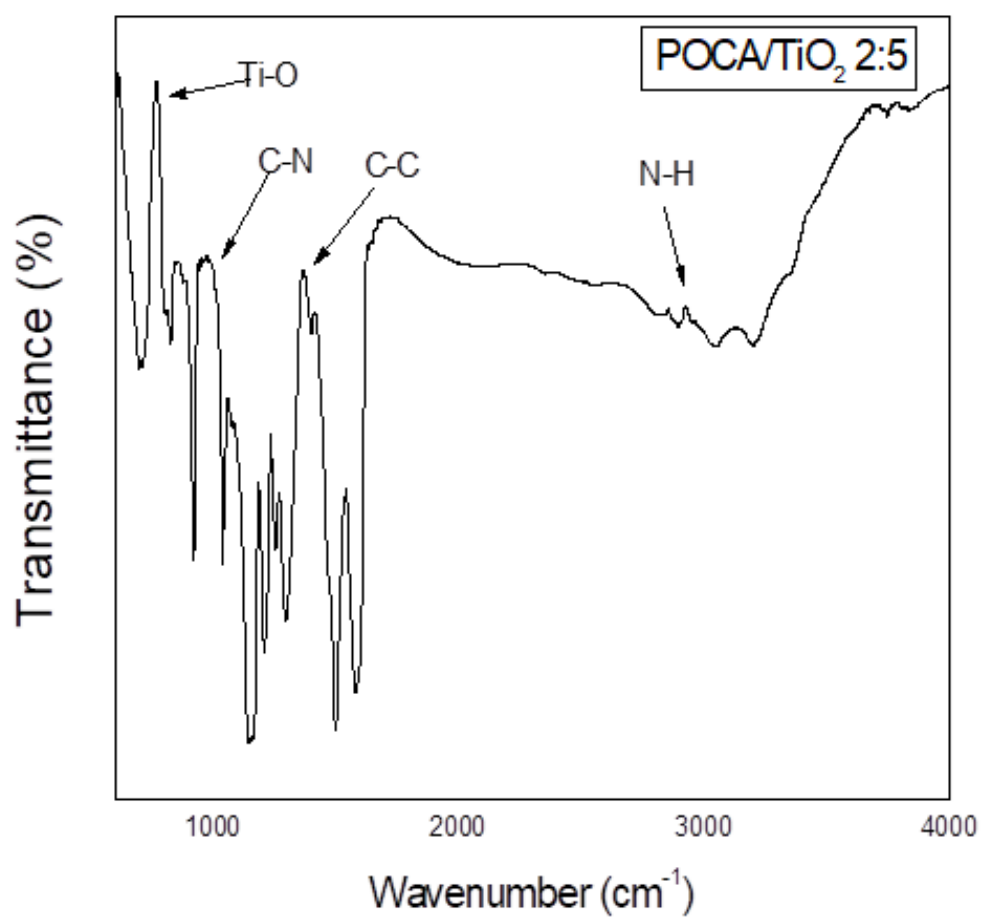
Fig 3.2 FTIR spectra of POCA/TiO₂ sample (S2)
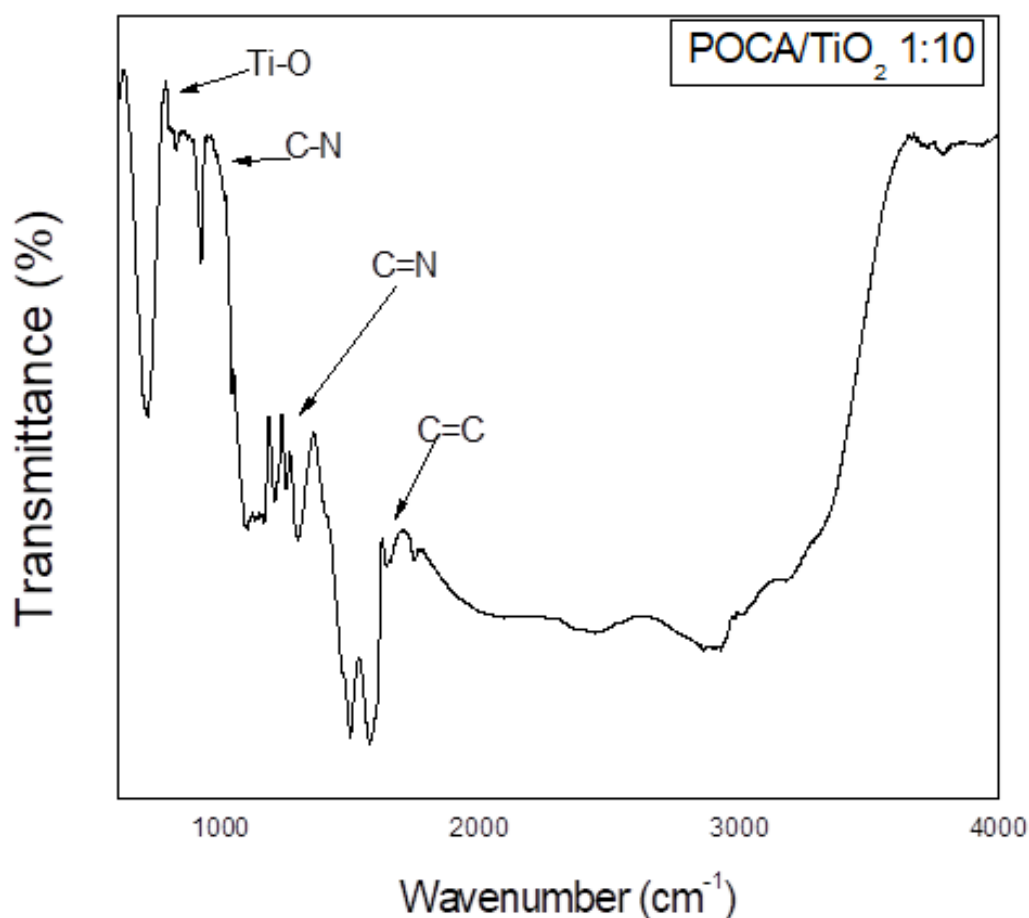
Fig 3.3 FTIR spectra of POCA/TiO₂ sample (S3)

3.2 X-ray diffraction of POCA/TiO₂ nanocomposite

To elucidate the structure of polyaniline and POCA/TiO₂ nanocomposite, FTIR analysis was carried out. Figure showed that the stretching mode of N-H group generated a peak at $3325 cm^{-1}$. The C=C and C=N stretching of benzenoid and quinoid units occurred at $1490 cm^{-1}$ and $1385 cm^{-1}$ respectively. On the other hand, C−N stretching of quinoid at $1100 cm^{-1}$, and C−N stretching of benzenoid at $1287 cm^{-1}$, was appeared for polyaniline in the FTIR spectra. The emeraldine form of polyaniline was confirmed by the presence of quinoid and benzenoid units. Same characteristic peaks were also found in POCA/TiO₂ nanocomposite that was exactly present in polyaniline FTIR spectra, but the intensity of peaks was changed due to the presence of titanium oxide nanoparticles.

Peaks were shifted to lower wavenumber which indicated the presence of titanium oxide affected the bond energies and electron densities of polyaniline in composite form. Results showed that the electron density of polyaniline was also increased (Naushad *et al.,* 2019).
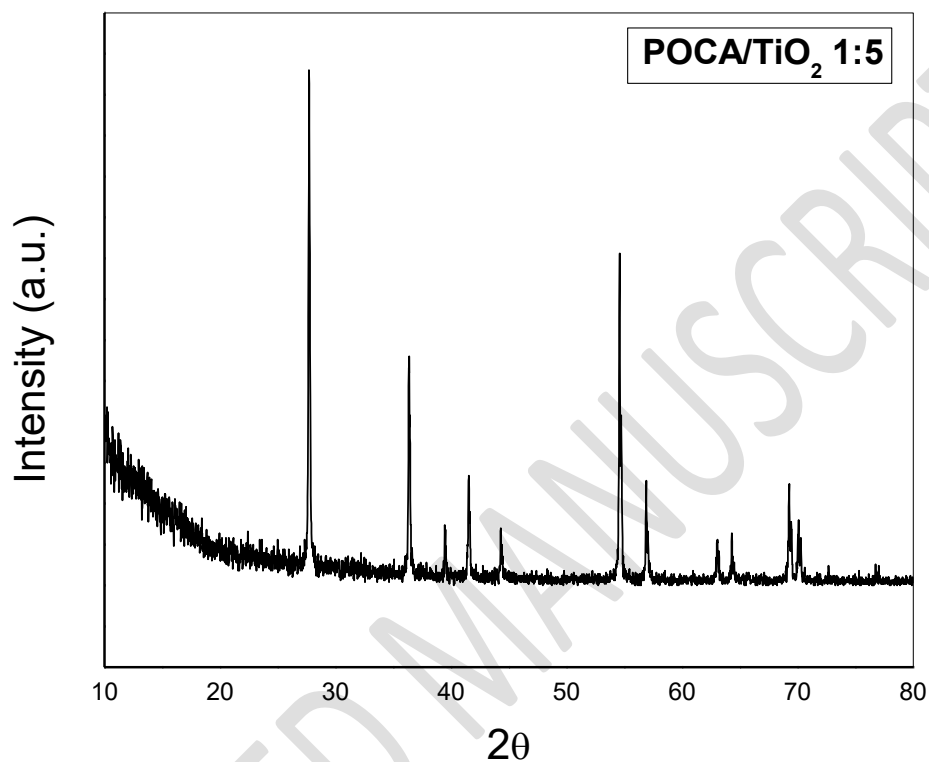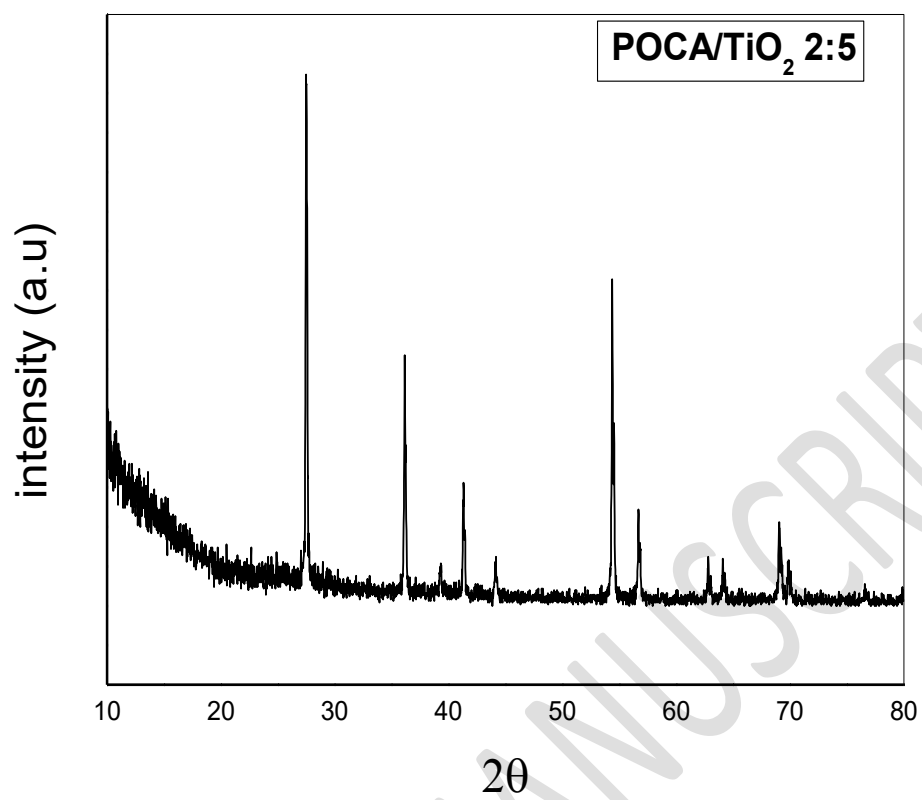

Fig 3.4 XRD spectra of POCA/TiO₂ sample (S1)

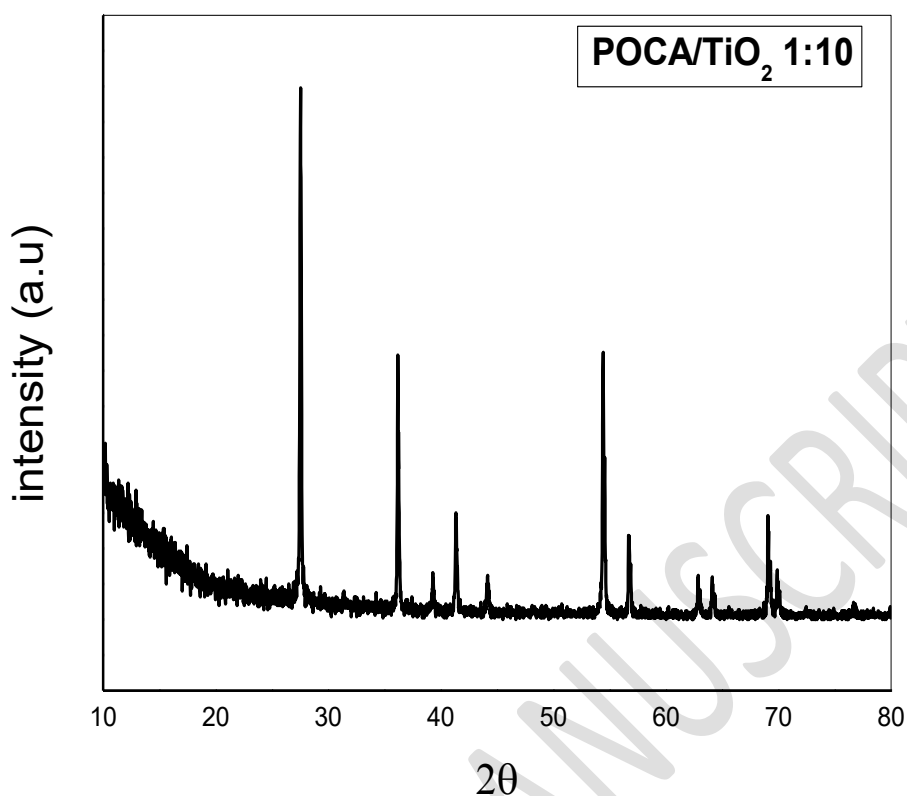**Fig 3.5 XRD spectra of POCA/TiO₂ sample (S2)**

Fig 3.6 XRD spectra of POCA/TiO₂ sample (S3)

XRD technique is used to determine the structure of different nanocomposites. Crystalline materials are characterized by XRD which is the most important non-destructive approach. By constructive interference of a monochromatic beam of X-rays, scattered XRD peaks were produced at different particular angles from every set of lattice planes in a compound. POCA/TiO₂ nanocomposite structures were examined by using of X-ray diffraction technique. XRD patterns of POCA/TiO₂ nanocomposites were shown in Fig. 3.4, 3.5, 3.6. Four different peaks were detected in the region of $2\theta = 16\text{-}26^\circ$, where the largest peak was around $2\theta = 18.1^\circ$ which imputed that the polymer chains of polyamine were perpendicular, parallel and repeated after several distances. The second peak that was present at $2\theta = 20^\circ$ as a characteristic peak. That indicated the close contact distance between the chains or the distance between the planes of the benzene rings by nearby chains. Additionally, the peak present at $2\theta = 24^\circ$ indicated that the polyaniline had very small degree of crystallinity and polyaniline chains were scattered in spaces

present between the planes. The XRD pattern of the POCA/TiO$_2$ nanocomposites indicated that there were very small peaks of titanium dioxide nanoparticles at $2\theta = 32\text{-} 38^{\circ}$. These peaks indicated that the molar ratio of TiO$_2$ was very small as compared to polyaniline. A peak at $2\theta = 32.5^{\circ}$ explained the crystallinity and wurtzite like hexagonal structure of titanium oxide (Eskizeybek *et al.,* 2012).

3.3 Scanning Electron Microscopy (SEM)

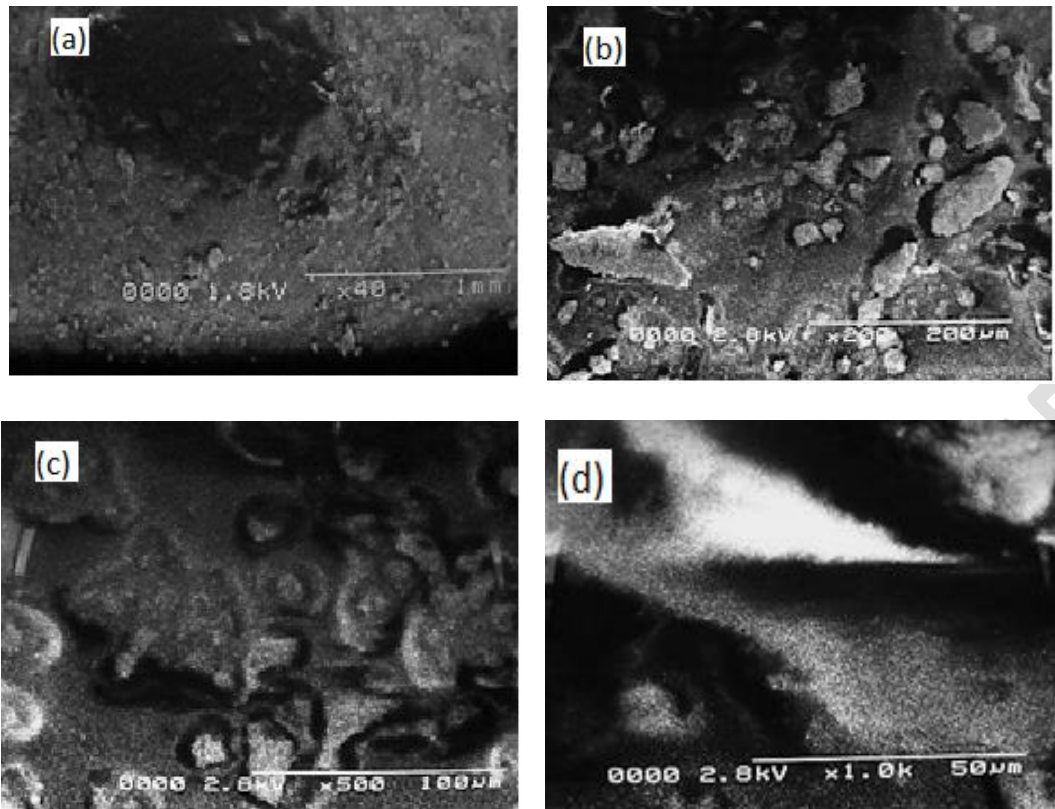**Fig. 3.7 SEM images of POCA/TiO$_2$ nanocomposites sample (S1) (1:5)**
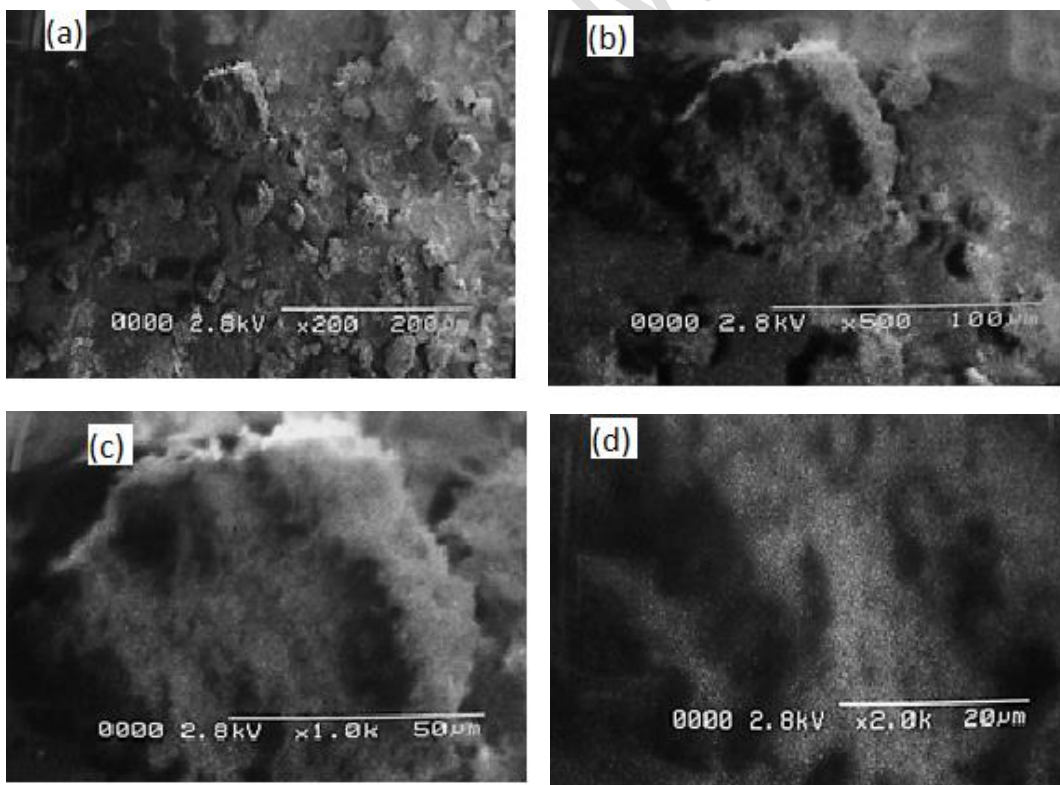

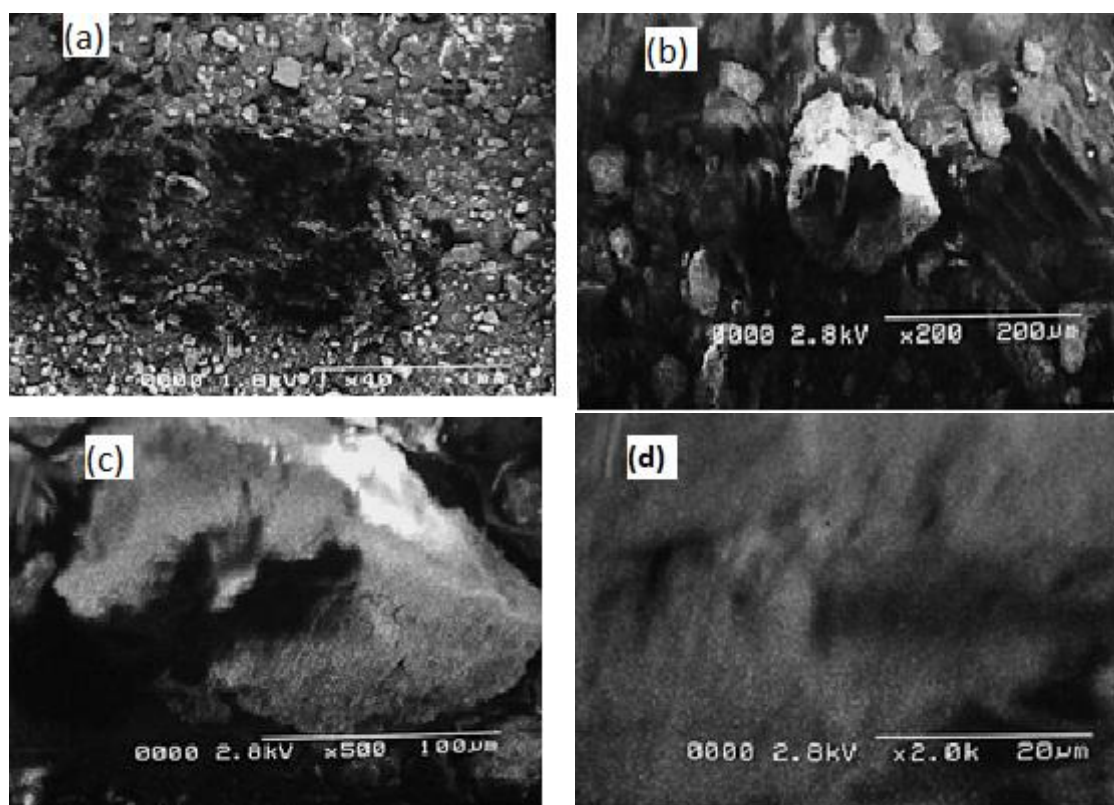**Fig. 3.8 SEM images of POCA/TiO$_2$ nanocomposites sample (S2) (2:5)**

Fig. 3.9 SEM images of POCA/TiO$_2$ nanocomposites sample (S3) (1:10)

The morphology of POCA/TiO$_2$ nanocomposites was investigated by the Scanning electron microscopic technique. Fig. 3.7, 3.8, 3.9 showed the SEM images of POCA/TiO$_2$ nanocomposites. These images showed the core-shell structure of nanocomposites. Irregular clusters were shown in these images which indicated the uniform dispersion of TiO$_2$ nanoparticles in the matrix of polyaniline. Multiparticle was grown after the formation of nanocomposite when polyaniline chains covered the nanoparticles of titanium dioxide. At low magnification, it was hard to observe the structure of TiO$_2$. These results explained the reason why the XRD spectrum of the POCA/TiO$_2$ nanocomposite showed peaks of hexagonal titanium oxide. After a deep study of these images, it was illustrated the morphology of POCA/TiO$_2$ nanocomposites and the uniform dispersibility of titanium oxide (Alishahi *et al.,* 2020).

4. Photocatalytic Activity

A homemade device was used to study the photodegradation process. The device contains a degradation chamber that is equipped for sunlight stimulation with a 500W Xe arc lamp and a 20W

neon lamp for ultraviolet light. The distance between the lamp and the upper surface of the sample was 16 cm. The photocatalytic process was checked out by degradation of direct yellow 50 sample solutions. To understand the dye degradation process, 100 ml sample of the sample solution of direct yellow 50 (5 mg/L) was taken in a 250 ml beaker. After the addition of 0.1 g of catalyst, the beaker was placed immediately in the degradation chamber carefully. The beaker containing mixture of both dye and catalyst was put on stirred for 1 h until equilibrium was attained. After intervals, a small portion of the solution was collected and centrifuged to analyze the degradation of direct yellow 50 with the help Ultraviolet-Visible spectrophotometer. The sample was tested after every 10 minutes interval to record the absorbance which showed the extent of degradation of target dye under the light. The process was continued up to 120 minutes till no significant change in the absorbance was observed. It was observed that the absorbance was decreased continuously with the time which confirmed the catalytic action occurred on the dye. So, the catalyst interacted with the dye to change it into different nontoxic substances (Tahiliani *et al.,* 2009).
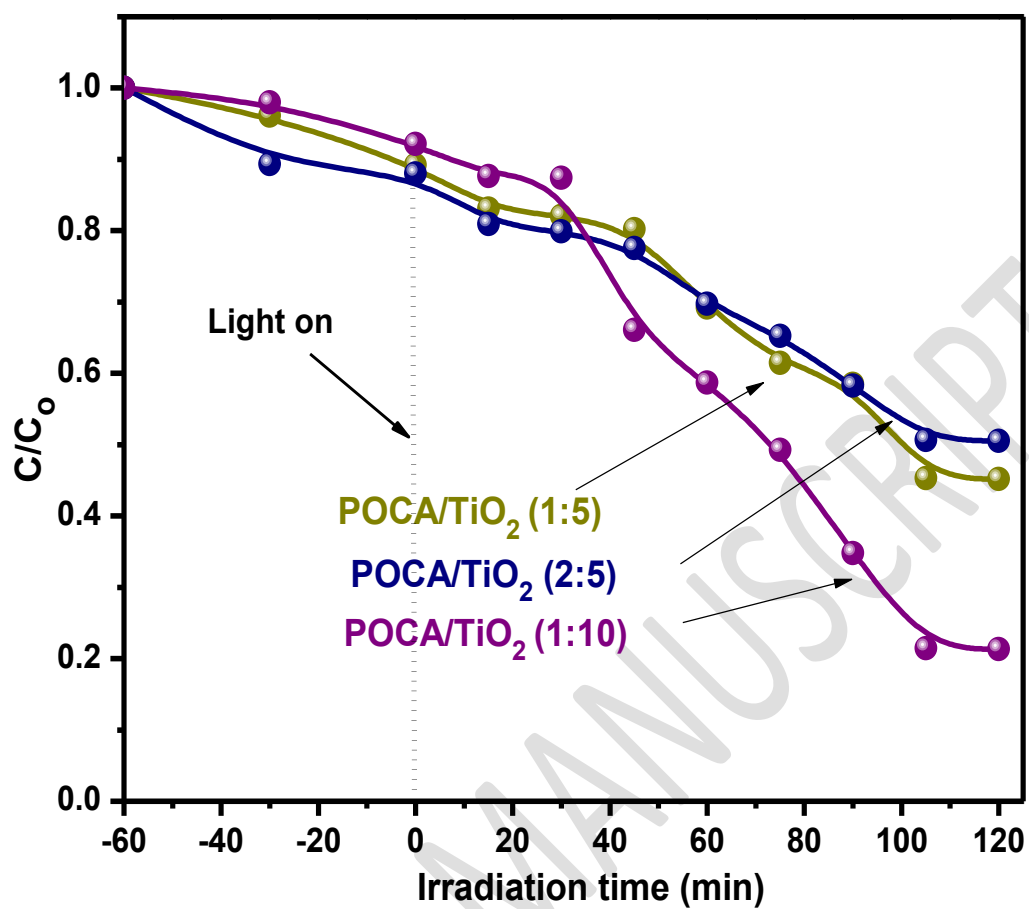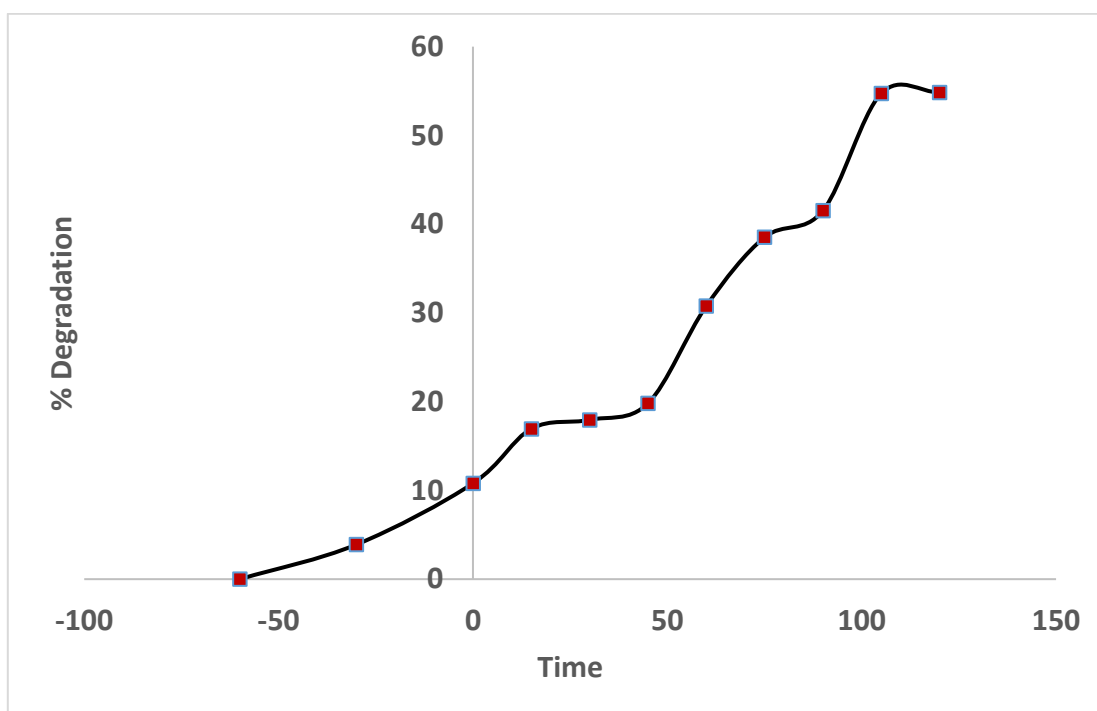
Fig. 4.1 Photocatalytic degradation of NCs

Fig 4.2 Percentage degradation efficiency of POCA/TiO$_2$ (S1)

The photodegradation of direct yellow 50 was observed under visible and ultraviolet light to evaluate the photocatalytic potential of the prepared nanocomposite (S1). The degradation of dye was detected after different intervals of time. It was observed that after 110 min, there was 54% of dye degradation by the nanocomposite (S1).
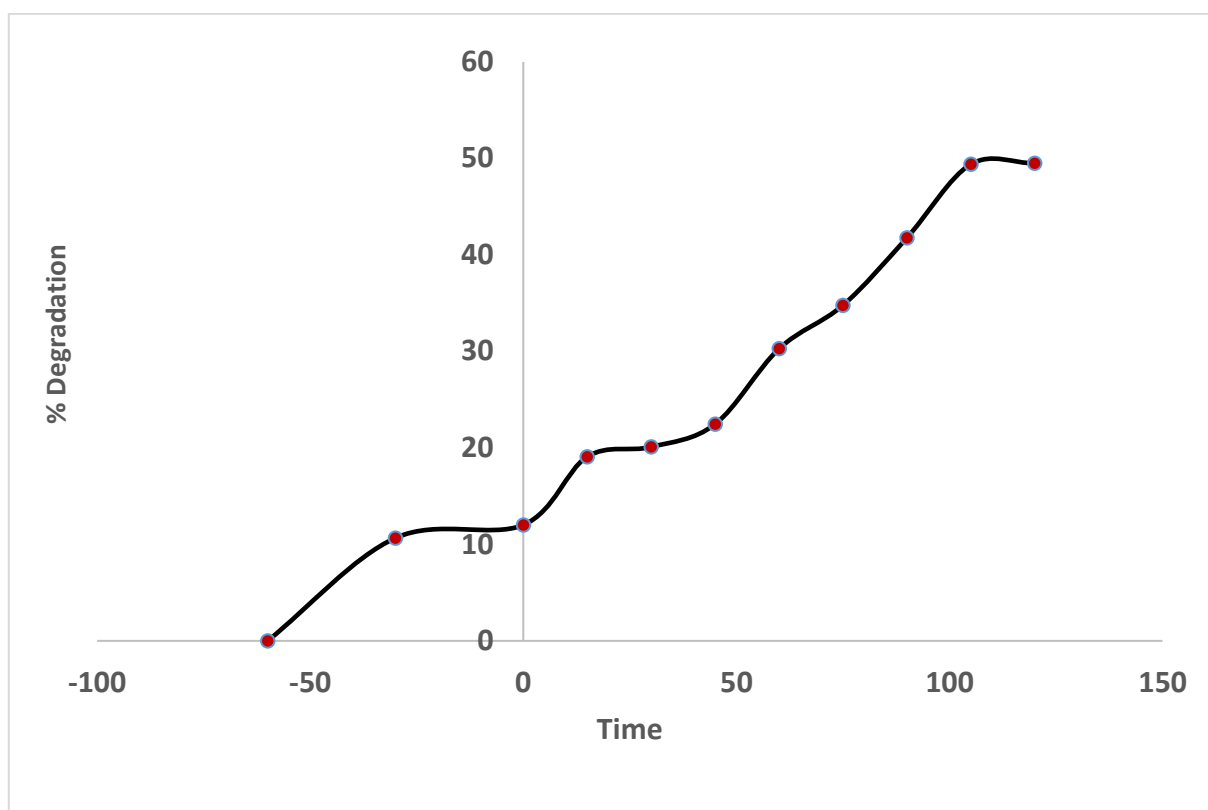
Fig 4.3 Percentage degradation efficiency of POCA/TiO₂ (S2)

The photodegradation of direct yellow 50 was observed under visible and ultraviolet light to evaluate the photocatalytic potential of the prepared nanocomposite (S2). The degradation of dye was checked after different intervals of time. It was observed that after 110 minutes, there was 49% of dye degradation by the nanocomposite (S2).
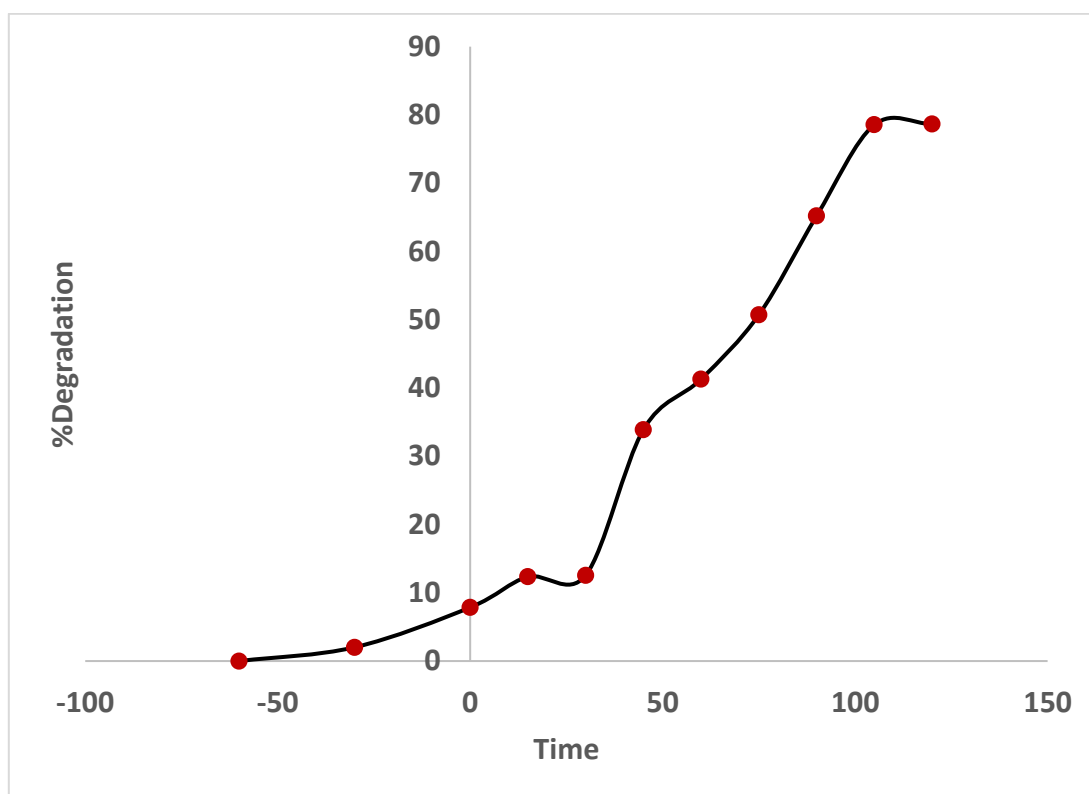
Fig 4.4: Percentage degradation efficiency of POCA/TiO$_2$ (S3)

The photodegradation of direct yellow 50 was detected under visible and ultraviolet light to study the photocatalytic potential of prepared nanocomposite (S3). This degradation of dye was evaluated after different intervals of time. It was observed that after 110 minutes there, was 78% of dye degradation by the nanocomposite (S3).

5. Conclusion

A series of POCA/TiO$_2$ nanocomposites were successfully prepared by varying the percentage of TiO$_2$ nanofiller in POCA matrix. That was also confirmed by different characterization techniques. The composites were then applied for photocatalytic degradation of direct yellow 50 dye. Among all the nanocomposites, the composite S3 (1:10) showed the highest photocatalytic degradation against DY50 under UV irradiation. This improvement was attributed to POCA which effectively improved the ability to transfer the photoexcited electrons. It also increased the absorption of light and degradation of dye by the composites. The catalytic activity of photocatalytic composite with

higher efficiency has excellent potential for environmental application for the degradation of other dyes as well.

REFERENCES

Ali, W., Ullah, H., Zada, A., Muhammad, W., Ali, S., Shaheen, S., Bilal, H. (2020). Synthesis of TiO₂ modified self-assembled honeycomb ZnO/SnO₂ nanocomposites for exceptional photocatalytic degradation of 2,4-dichlorophenol and bisphenol A. *Science of the Total Environment, 746*, 141291.

Alishahi, M., Khorram, M., Asgari, Q., Davani, F., Goudarzi, F., Emami, A., Zomorodian, K. (2020). Glucantime-loaded electrospun core-shell nanofibers composed of poly (ethylene oxide)/gelatin-poly(vinyl alcohol)/chitosan as dressing for cutaneous leishmaniasis. *International journal of biological macromolecules, 163*, 288-297.

Badvi, K., & Javanbakht, V. (2021). Enhanced photocatalytic degradation of dye contaminants with TiO₂ immobilized on ZSM-5 zeolite modified with nickel nanoparticles. *Journal of Cleaner Production, 280*, 124518.

Barzegar, M. H., Sabzehmeidani, M. M., Ghaedi, M., Avargani, V. M., Moradi, Z., Roy, V. A., & Heidari, H. (2021). S-scheme heterojunction g-C₃N₄/TiO₂ with enhanced photocatalytic activity for degradation of a binary mixture of cationic dyes using solar parabolic trough reactor. *Journal of Chemical Engineering Research Design, 174*, 307-318.

Belal, R. M., Zayed, M. A., El-Sherif, R. M., & Ghany, N. A. A. (2021). Advanced electrochemical degradation of basic yellow 28 textile dye using IrO₂/Ti meshed electrode in different supporting electrolytes. *Journal of Electroanalytical Chemistry, 882*, 114979.

Chen, S., Takata, T., & Domen, K. (2017). Particulate photocatalysts for overall water splitting. *Nature Reviews Materials, 2*(10), 1-17.

Eskizeybek, V., Sarı, F., Gülce, H., Gülce, A., & Avcı, A. (2012). Preparation of the new polyaniline/ZnO nanocomposite and its photocatalytic activity for degradation of methylene

blue and malachite green dyes under UV and natural sun lights irradiations. *Applied Catalysis B: Environmental, 119*, 197-206.

Eslami, A., Kashani, M. R. K., Khodadadi, A., Varank, G., Kadier, A., Ma, P.-C., Ghanbari, F. (2021). Sono-peroxi-coagulation (SPC) as an effective treatment for pulp and paper wastewater: Focus on pH effect, biodegradability, and toxicity. *Journal of Water Process Engineering, 44*, 102330.

Huang, J., Shi, Y., Zeng, G., Gu, Y., Chen, G., Shi, L., Zhou, J. (2016). Acyl-homoserine lactone-based quorum sensing and quorum quenching hold promise to determine the performance of biological wastewater treatments: An overview. *Chemosphere, 157*, 137-151.

Kaounides, L., Yu, H., & Harper, T. (2007). Nanotechnology innovation and applications in textiles industry: current markets and future growth trends. *Materials Technology, 22*(4), 209-237.

Konstantinou, I. K., & Albanis, T. A. (2004). TiO_2-assisted photocatalytic degradation of azo dyes in aqueous solution: kinetic and mechanistic investigations: An review. *Applied Catalysis B: Environmental, 49*(1), 1-14.

Lee, K. X., Shameli, K., Yew, Y. P., Teow, S.-Y., Jahangirian, H., Rafiee-Moghaddam, R., & Webster, T. J. (2020). Recent developments in the facile bio-synthesis of gold nanoparticles (AuNPs) and their biomedical applications. *International journal of nanomedicine, 15*, 275.

Madhav, S., Ahamad, A., Singh, P., & Mishra, P. K. (2018). A review of textile industry: Wet processing, environmental impacts, and effluent treatment methods. *Environmental Quality Management, 27*(3), 31-41.

Naushad, M., Sharma, G., & Alothman, Z. A. (2019). Photodegradation of toxic dye using Gum Arabic-crosslinked-poly (acrylamide)/Ni $(OH)_2$/FeOOH nanocomposites hydrogel. *Journal of Cleaner Production, 241*, 118263.

Nguyen, M. B., Le, G. H., Nguyen, T. D., Nguyen, Q. K., Pham, T. T., Lee, T., & Vu, T. A. (2021). Bimetallic Ag-Zn-BTC/GO composite as highly efficient photocatalyst in the photocatalytic

degradation of reactive yellow 145 dye in water. *Journal of Hazardous Materials, 420*, 126560.

Nguyen, T. K. A., Pham, T.-T., Nguyen-Phu, H., & Shin, E. W. (2021). The effect of graphitic carbon nitride precursors on the photocatalytic dye degradation of water-dispersible graphitic carbon nitride photocatalysts. *Journal of Applied surface science, 537*, 148027.

Noman, M., Shahid, M., Ahmed, T., Niazi, M. B. K., Hussain, S., Song, F., & Manzoor, I. (2020). Use of biogenic copper nanoparticles synthesized from a native Escherichia sp. as photocatalysts for azo dye degradation and treatment of textile effluents. *Environmental Pollution, 257*, 113514.

Oon, Y.-S., Ong, S.-A., Ho, L.-N., Wong, Y.-S., Oon, Y.-L., Lehl, H. K., & Thung, W.-E. (2021). Innovative baffled microbial fuel cells for azo dye degradation: Interactive mechanisms of electron transport and degradation pathway. *Journal of Cleaner Production, 295*, 126366.

Ramamoorthy, S., Das, S., Balan, R., & Lekshmi, I. (2021). TiO_2-ZrO_2 nanocomposite with tetragonal zirconia phase and photocatalytic degradation of Alizarin Yellow GG azo dye under natural sunlight. *Journal of Materials Today: Proceedings*.

Rani, M., & Shanker, U. (2020). Efficient photocatalytic degradation of Bisphenol A by metal ferrites nanoparticles under sunlight. *Environmental Technology & Innovation, 19*, 100792.

Rouzafzay, F., Shidpour, R., Al-Abri, M. Z., Qaderi, F., Ahmadi, A., & Myint, M. T. Z. (2020). Graphene and ZnO nanocompound for short-time water treatment under sun-simulated irradiation: Effect of shear exfoliation of graphene using kitchen blender on photocatalytic degradation. *Journal of Alloys and Compounds, 829*, 154614.

Sarkar, B., Chakrabarti, K., Das, K., & De, S. (2012). Optical and ferroelectric properties of ruthenium-doped $BaTiO_3$ nanocubes. *Journal of Physics D: Applied Physics, 45*(50), 505304.

Tahiliani, M., Koh, K. P., Shen, Y., Pastor, W. A., Bandukwala, H., Brudno, Y., Aravind, L. (2009). Conversion of 5-methylcytosine to 5-hydroxymethylcytosine in mammalian DNA by MLL partner TET1. *Science, 324*(5929), 930-935.

Vijayaraghavan, T., Althaf, R., Babu, P., Parida, K., Vadivel, S., & Ashok, A. M. (2021). Visible light active $LaFeO_3$ nano perovskite-RGO-NiO composite for efficient H_2 evolution by photocatalytic water splitting and textile dye degradation. *Journal of Environmental Chemical Engineering, 9*(1), 104675.

List of Figures

List of Tables